Available online at www.sciencedirect.com
ScienceDirect
Journal of the European Ceramic Society 28 (2008) 1205–1212
www.elsevier.com/locate/jeurceramsoc

Dispersion of nano-sized $BaTiO_3$ powders in nonaqueous suspension with phosphate ester and their applications for MLCC

Li Wen Chu [a,*], Kuraganti Niranjan Prakash [a], Men-Tsuan Tsai [a], I-Nan Lin [b]

[a] *Research and Development Division, Walsin Technology Corporation, Kaohsiung 300, Taiwan, ROC*
[b] *Department of Physics, Tamkang University, Tamsui 251, Taiwan, ROC*

Received 14 February 2007; received in revised form 15 October 2007; accepted 26 October 2007
Available online 11 January 2008

Abstract

The stability of nano-sized $BaTiO_3$ nonaqueous suspension with different phosphate ester surfactants was investigated. Among the three phosphate esters (mono-alkyl, di-alkyl and ethoxy types), the 2-ethoxy ethyl dihydrogen (1EO-) phosphate esters show not only better coverage over the nano-$BaTiO_3$ powders, but also superior dispersion for the suspension. Contrary to the conventional 200 nm-$BaTiO_3$ suspensions, which need longer carbon-chain phosphate esters surfactant for dispersing the $BaTiO_3$ powders, the 50 nm-$BaTiO_3$ suspensions require shorter carbon-chain phosphate esters surfactant for dispersing them. Multilayer ceramic capacitors (MLCC) made of 50 nm-$BaTiO_3$ suspensions contain ultra-thin ceramic layer (2.6–2.8 μm), which shows the larger capacitance and superior breakdown voltage than those made of 200 nm-$BaTiO_3$ powders.

Keywords: Suspensions; Tape-casting; Nanocomposites; $BaTiO_3$; Capacitors

1. Introduction

Barium titanate ($BaTiO_3$) perovskite oxides are widely used for manufacturing multilayer ceramic capacitors (MLCCs)[1,2] due to their marvelous dielectric properties. With the trend for increasing the volumetric efficiency of MLCCs, the thickness of the ceramic capacitor layer needs to be reduced (<5 μm in thickness), which call for the utilization of the nano-sized $BaTiO_3$ powders[3] as starting materials. The dispersion behavior of nano-sized $BaTiO_3$ powders in a solvent is totally different from that of the conventional slurry made of submicron $BaTiO_3$ powders (~200 nm). The dispersion of the nano-sized $BaTiO_3$ powders in a solvent is a challenging problem needs to be addressed for preparing the stabilized suspension used in ultra-thin ceramic tape fabrication process.[4–11] On the other hand, phosphate ester is a commonly used dispersant for various ceramic tape,[12–16] especially for $BaTiO_3$ materials.[17–19] The phosphate esters contain hydroxy group, which are ionized to form negatively charged oxygen[18,20] and react with ceramic powders electrostatically in the solvent. However, the chemical variety of phosphate esters influences the dispersion behavior of the slurry in a complicated manner.

In this study, phosphate esters with different molecular structure, including mono-alkyl group, di-alkyl group and mono-ethoxy group, were synthesized. They were utilized as surfactants for dispersing the ultra-fine $BaTiO_3$ powders (50 nm). The influence of molecular structure of phosphate esters on the dispersion characteristics of the nano-sized $BaTiO_3$ suspension is systematically studied. The benefit of using nano-sized $BaTiO_3$ powders for fabricating the multilayer ceramic capacitors was illustrated.

2. Experimental

2.1. Powder and chemicals

High purity ultra-fine $BaTiO_3$ powders prepared by hydrothermal process were used as starting materials (HPB-1000 (50 nm) and HPB-1200 (200 nm), TPL Inc., USA). The nano-sized $BaTiO_3$ powders were dried at 120 °C for 6 h to remove the moisture adsorbed on the powders. The phosphate esters were dissolved in 1-methoxy-2-propanol (>99%, Fluka, Switzerland) to serve as surfactant. The solvents were boiled with the desiccating agent before mixing with powders to avoid

* Corresponding author.
E-mail address: g873120@yahoo.com.tw (L.W. Chu).

0955-2219/$ – see front matter © 2007 Elsevier Ltd. All rights reserved.
doi:10.1016/j.jeurceramsoc.2007.10.015

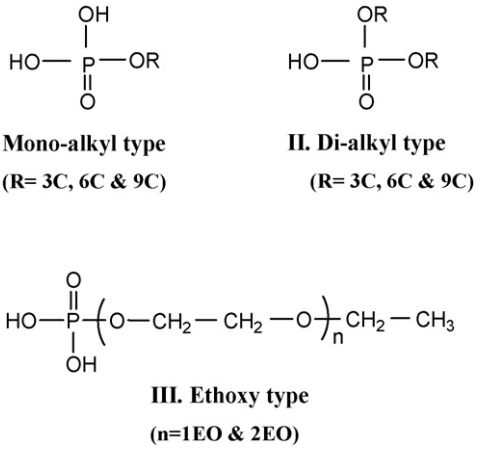

Fig. 1. Chemical structure of various synthesized phosphate esters.

water contamination in the preparation of suspension. The phosphate esters (~5 wt% w.r.t. $BaTiO_3$ powders) and the nano-$BaTiO_3$ powders were added in the solvent sequentially with thorough mixing to form the suspensions with high solid content (~40 wt%).

2.2. Synthesis of phosphate esters

Three types of anionic phosphate esters: mono-alkyl, di-alkyl, and ethoxy phosphates, with the structure shown in Fig. 1, were prepared. Mono-alkyl and ethoxy phosphates were prepared by stirring the chosen alcohols with pyrophosphoric acid.[21,22] These reactions proceeded as follows:

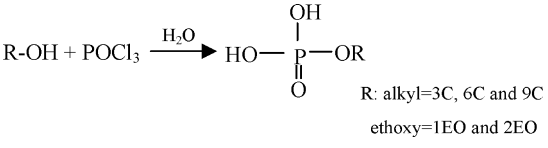

(1)

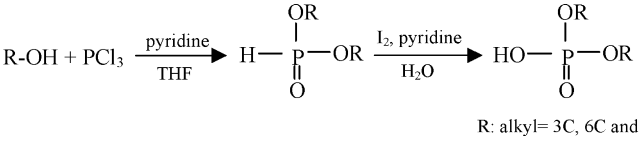

(2)

The pyrophosphoric acid (>99%, Riedal-deHaën, Switzerland) was mixed with the corresponding alcohols in molar ratio of 1:1.05 for syntheses of mono-alkyl phosphate esters. The corresponding alcohols were ethanol (reagent grade, Riedal-deHaën, Switzerland), 1-propanol (>99.8%, Tedia, America), hexanol (Perified, J. T. Baker, America), nonanol (>98%, Fisher, America) and dodecanol (>98%, Acros, Belgium), respectively. For synthesizing the ethyl-type phosphate esters, the utilized alcohols were 2-(2-ethoxyethoxy) ethanol (99%, Tedia, America) and 2-ethoxy ethanol (99%, Tedia, America). The deionized water was added into the reactant in proper ratio to initiate hydrolysis.

In contrast, the higher activity reagent PCl_3 was replaced with $POCl_3$ and the corresponding alcohol to form the di-*n*-alkyl phosphates.[22] The di-alkyl phosphate esters were prepared by stirring phosphorus trichloride (>99.8%, Riedal-deHaën, Switzerland) with the corresponding alcohol and pyridine (99.9%, Tedia, America) in the molar ratio of 1:2.1:2.1 for 1 h in sufficient tetrahydrofuran (THF) (>99%, Tedia, USA), followed by reaction with I_2 solution. Finally, the de-ionized water was added to initiate the hydrolysis. The structures of prepared phosphate esters were confirmed by ^1H NMR spectrometer (UNITYINOVA 500, Varian, USA) and FTIR analysis (FTS-40, Bio-Rad, UK). The typical spectra were shown in Fig. 2(a) and (b).

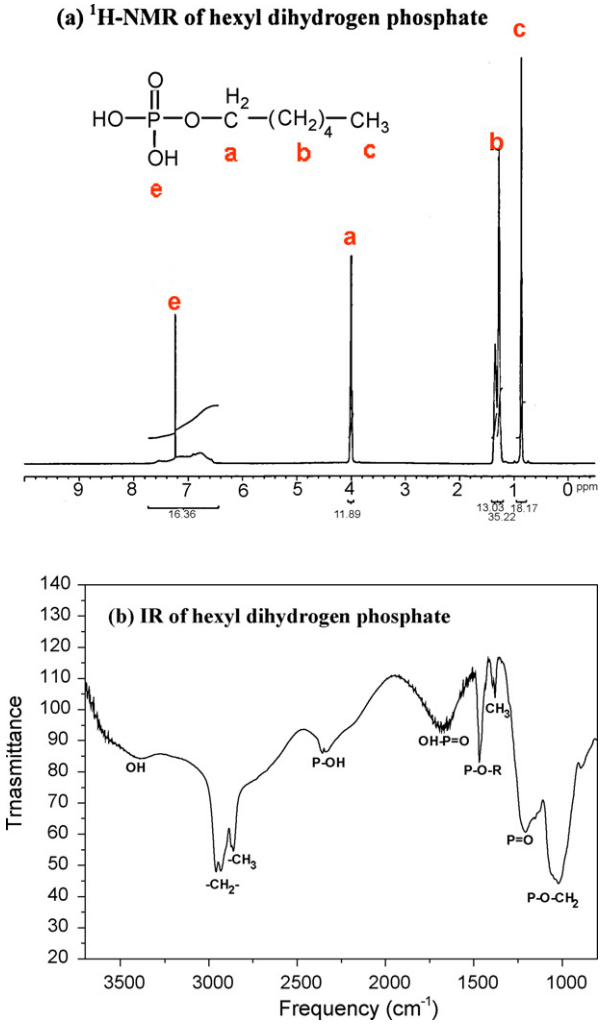

Fig. 2. (a) ^1H NMR spectra and (b) FTIR spectra of synthesized phosphate ester (i.e., hexyl dihydrogen phosphate).

2.3. Preparation and characterization of suspensions and MLCC

Although ethanol works as solvent very well for preparing the $BaTiO_3$ slurry in tape-casting process[18,19] for conventional micron-sized $BaTiO_3$ powders, it is inadequate for nano-sized $BaTiO_3$ powders. Table 1 compares the important parameters of ethanol and 1-methoxy-2-propanol, including boiling point, dielectric constant and viscosity, and characteristics of the solid

Table 1
The characteristics of solid suspensions without the dispersants addition

Solvents	Solvent properties			Suspension properties		
	Boiling point (°C)	Dielectric constant	Viscosity (cp)	Zeta (mV)	Sediment (min)	Particle size (nm)[a]
Ethanol	78	24.0	1.00	4.92	45	420
1-Methoxy-2-propanol	120	–	2.4	1.94	>60	138

[a] The average particle size distribution of 2.5 wt% solid suspension was stored statically for 30 min and analyzed by dynamic light scattering.

suspensions with 2.5 wt% $BaTiO_3$ by dispersing in both the solvents, respectively.

Table 1 indicates that the sedimentation time of the 1-methoxy-2-propanol based suspension is more than 60 min, which is markedly superior to the ethanol based one with 45 min sedimentation time. It should be noted that the sedimentation time is designated as the time when the powders settled to a height of 2 cm in the sealed glass tube. The average size of agglomerates for the 1-methoxy-2-propanol based suspension is 138 nm, which is smaller than the ethanol based one (420 nm). Without any surfactant addition, the nano-sized $BaTiO_3$ is dispersed better in 1-methoxy-2-propanol than that in ethanol. Therefore, we can conclude that 1-methoxy-2-propanol to replace ethanol as solvent in this study.

The SEM micrographs show in Fig. 3(a) and (b) for ethanol and 1-methoxy-2-propanol based suspensions, respectively. The above figures clearly illustrate that the nano-sized $BaTiO_3$ powders is well dispersed in 1-methoxy-2-propanol suspension, but agglomeration is observed in ethanol suspension. The zeta potential of $BaTiO_3$ in ethanol (4.92 mV) is larger than that of $BaTiO_3$ in 1-methoxy-2-proponal (1.94 mV), whereas the viscosity of 1-methoxy-2-proponal based suspension ($\eta = 2.4$ cp) is larger than that of the ethanol based suspension ($\eta = 1.0$ cp). The viscosity of solvent seems to influence the dispersion behavior of the nano-sized $BaTiO_3$ suspensions more profoundly than zeta potential.

The suspensions were prepared by mixing $BaTiO_3$ powder (2.5–40 wt%) with 1-methoxy-2-propanol solvents, which contain various amounts of phosphate esters. The slurries were de-agglomerated by using a high efficiency centrifugal mixer (Tai-Yiaeh Inc., Taiwan) for 1 h. The particle size of the powders in suspension were measured by using dynamic light scattering apparatus (DLS) (Zetasizer 1000HSA, Malvern, UK) for low solid-content suspension, and using acoustic type particle sizer (Ascoutosizer II, Colloidal dynamics, USA) for 40 wt% solid-content suspension. The zeta potential of $BaTiO_3$ in the suspension was measured by using an electro-acoustics type zeta potential analyzer (Zeta-probe, Colloidal dynamic, USA). The rheological behavior of suspension was measured by a viscometer (LVDV-I^+, Brookfield, USA) with LV-3 spindle at 50 rpm rotation rate.

To examine the adsorption behavior of phosphate esters onto the nano-$BaTiO_3$ powders, the stabilized suspension was centrifuged (3000 rpm for 10 min) to separate the powders from the suspension. The powders were slowly dried at room temperature. The adsorbed phosphate esters on the powders were analyzed by using diffuse reflectance infrared Fourier transform spectroscopy (DRIFTS) (DA83, Bomem, Canada). Meanwhile, the residual concentration of phosphate esters in the solvent was analyzed by the induced coupled plasma analyzer (ICP) (Vista-mpx, Varian, USA). The droplets of $BaTiO_3$ suspension on silicon substrate were dried in an oven and the morphology of $BaTiO_3$ agglomerates were examined by using scanning electron microscopy (6700F, JEOL, Japan).

After the preparation of high solid content suspension (40 wt% 50 nm-$BaTiO_3$) with 2-ethoxy ethyl (1EO-) phosphate (5 wt% w.r.t. $BaTiO_3$ powders) in 1-methoxy-2-propanol, the organic additives (polyvinyl butyral (PVB, Butvar, USA) and

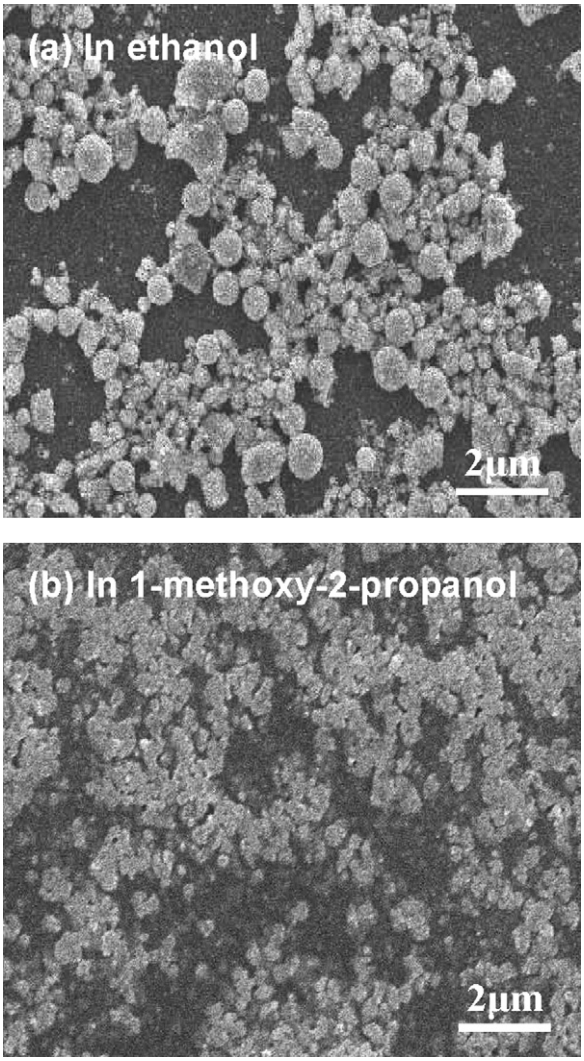

Fig. 3. SEM micrographs of the (a) ethanol and (b) 1-methoxy-2-propanol based suspensions with pH ~ 7, which were dried slowly from the droplets on a substrate.

di-octyl phthalate (DOP, Fluka, Switzerland)) were added to the $BaTiO_3$ suspension in the weight ratio of 9:2:1 (suspension/PVB/DOP) to adjust the viscosity of the slurry followed by ball-mixing for 10 h. The slurry was used to produce the ultra-thin ceramic foil (2.6–2.8 μm) via a tape-casting machine (Hirano, Japan) and followed by standard multilayer ceramic process to fabricate the MLCC devices. The breakdown voltage and capacitance of the MLCC device were analyzed by electric voltage tester (9052, Chen-Hwa, Taiwan) and capacitance meter (HP, 4278A, USA), respectively.

3. Results and discussion

3.1. Adsorption behavior of phosphate esters

The phosphate esters developed negative charges when dissolved in the solvent, and are readily attached to the $BaTiO_3$ powders. The zeta potential of $BaTiO_3$ powders is reduced due to the adsorption of the surfactant, designated as "differential zeta", is a good estimation for the coverage of particles by the phosphate esters. The "differential zeta" of 10 wt% $BaTiO_3$ suspensions in 1-methoxy-2-propanol, which contain 2 wt% phosphate esters (w.r.t. $BaTiO_3$ powders), is illustrated in Fig. 4. The "differential zeta" decreases with the increasing carbon chain length (nC-) of phosphate esters. Mono-alkyl type phosphate esters show larger "differential zeta" than di-alkyl type ones, implying that the proportion of adsorption for mono-alkyl type phosphate esters is larger than that of di-alkyl type phosphate esters.

The $BaTiO_3$ powders obtained by centrifugation of suspension and were analyzed by DRIFTS to investigate the coverage of the phosphate esters. Typical DRIFRS pattern is shown in Fig. 5(a). Five absorption peaks are observed at: 840 cm^{-1} (Ba–Ti–O), 1150 cm^{-1} (C–O), 1450 cm^{-1} (CH_2, CH_3), 1300 cm^{-1} (P=O) and 1700 cm^{-1} (HO–P=O). The HO–P=O peak at 1700 cm^{-1} indicates the adsorption of mono/di-alkyl type phosphate esters on the $BaTiO_3$. Furthermore, the residual phosphorus in the solvent was quantitatively analyzed by induction couple plasma (ICP) technique after the $BaTiO_3$ (BT) powders were centrifugally separated from stabilized suspension. The amount of phosphate ester adsorbed on $BaTiO_3$ powders (A_s) was estimated as the difference between the phosphate ester contained in the solvent and the amount of phosphate ester added (C_e). The C_e/A_s was then plotted against C_e, which leads to monolayer absorption of phosphate ester C_m:

$$\frac{C_e}{A_s} = \frac{C_e}{C_m} + \frac{k}{C_m} \quad (3)$$

Typical plot is shown in Fig. 5(b), which fit to a straight line and the slope represents the reciprocal of monolayer adsorption of phosphate ester ($1/C_m$) according to the Langmuir monolayer adsorption analysis.[23] The C_m of phosphate ester decreases from mono-propyl ($(C_m)_{3C-} = 17.85$ mg/gm BT) to mono-hexyl ($(C_m)_{6C-} = 16.39$ mg/gm BT), implying that the increase in the alkyl length of phosphate ester leads to the decrease in proportion of adsorption. The smaller C_m-values

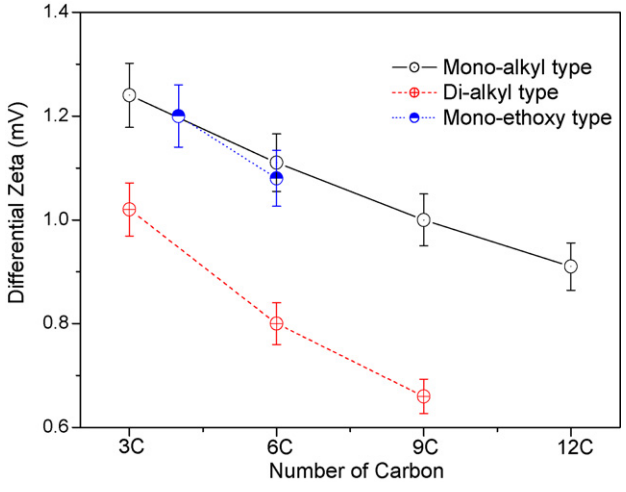

Fig. 4. Variation of differential zata, the decrease in zeta potential of $BaTiO_3$ as the phosphate ester was adsorbed onto the $BaTiO_3$ particles dispersing in 1-methoxy-2-propanol, with the number of carbons in the phosphate esters.

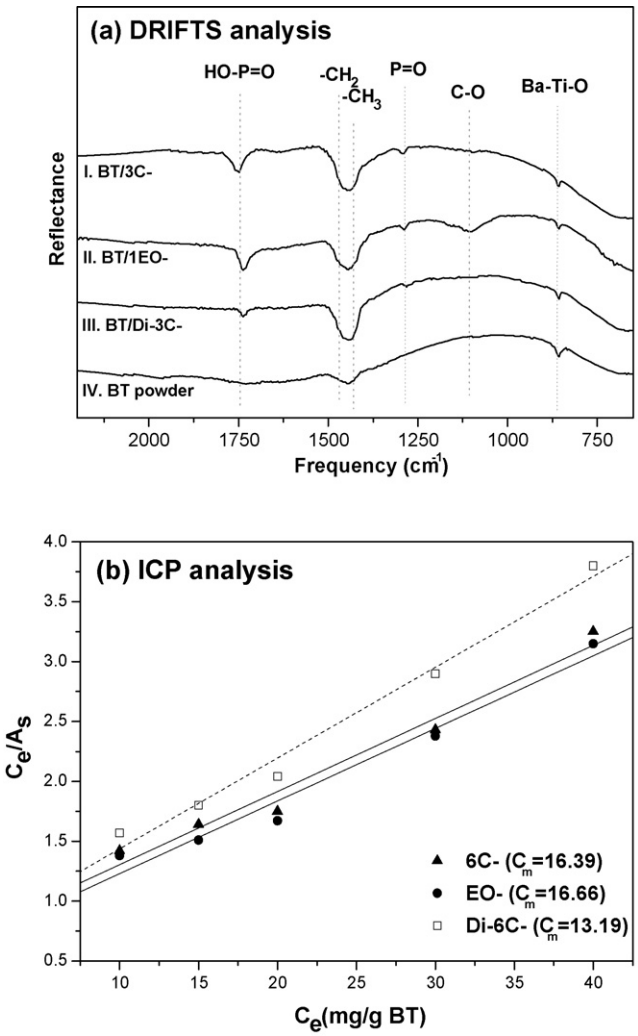

Fig. 5. (a) The diffuse reflectance FTIR spectra of the selected phosphate ester coated $BaTiO_3$ particles; (b) The Langmiur monolayer adsorption analysis for calculating the adsorption concentration of phosphate ester (C_m) onto $BaTiO_3$ particles in ethanol determined by ICP.

Table 2
Sedimentation time (min) of $BaTiO_3$ suspensions with different particle size of $BaTiO_3$ and phosphate esters

	Non-addition		Surfactants of phosphate esters							
	Zeta (mV)	Sediment (min)	Alkyl			Di-alkyl			Ethoxy	
			3C-	6C-	9C-	Di-3C-	Di-6C-	Di-9C-	EO-	2EO-
$BaTiO_3$ (50 nm)	4.05	45	60	55	30	90	60	S	110	85
$BaTiO_3$ (200 nm)	3.02	25	30	45	45	40	50	55	45	70

S: the slurry status of the powder suspension.

of di-alkyl type phosphate esters ((C_m)$_{Di\text{-}3C\text{-}}$ = 15.15 mg/gm BT and (C_m)$_{Di\text{-}6C\text{-}}$ = 13.19 mg/gm BT) show that di-alkyl type phosphate esters (Di-3C- and Di-6C-) have lower adsorption than the mono-alkyl type phosphate esters (3C- and 6C-). The ethoxy type phosphate esters show the same degree of adsorption as mono-alkyl type phosphate esters (i.e., (C_m)$_{1EO\text{-}}$ = 16.66 mg/gm BT). These results are in accord with the qualitative analysis in "differential zeta".

3.2. Suspension characteristics

A high solid content of $BaTiO_3$ suspension (50 nm, 40 wt%) containing phosphate esters (5 wt% w.r.t. powders) in 1-methoxy-2-propanol was prepared. The sedimentation time of $BaTiO_3$ suspension is smaller than 45 min when no surfactant was added. Table 2 (first row) shows that the dispersion of suspensions improves markedly due to the addition of mono-alkyl phosphate surfactants with carbon-chain smaller than hexyl (6C-). As the longer carbon-chain type of mono-alkyl phosphate esters (9C- and 12C-) added, the sedimentation time reduced instead. Therefore, the excess length of alkyl chain in phosphate esters can hinder the adsorption of surfactants onto the nano-sized $BaTiO_3$ powders, which degrades the dispersion behavior of the suspension. Similar phenomenon was also observed when the di-alkyl phosphate surfactants were used. It is interesting that the di-alkyl type phosphate esters exhibit better sedimentation behavior for the suspension, although it does not cover the $BaTiO_3$ powders as well as the mono-alkyl type one. We have observed that the 2-ethoxy ethyl (1EO-) phosphate ester contains carbon-chain larger than the mono-propyl (3C-) phosphate ester and enhances the dispersion behavior much better than the mono-alkyl type (3C-) phosphate ester. The beneficial effect of phosphate ester addition on dispersing nano-$BaTiO_3$ powders in 1-methoxy-2-propanol suspension is demonstrated in Fig. 6(a) and (b).

Fig. 7(a) shows the variation of viscosity of the suspensions with the powder content, containing three kinds of phosphate esters (3C, Di-3C and 1EO-) in 1-methoxy-2-propanol. The viscosity of the suspension increases with the powder content. For the suspension containing 40 wt% $BaTiO_3$ powders, the viscosity of suspension in 1-methoxy-2-propanol rapidly increases due to the occurrence of agglomerates. The ethoxy type surfactant is more effective in maintaining the suspension at low viscosity. On the other hand, it is known that the sedimentation will obviously occur when the particle size of agglomeration increases larger than 1 μm, which should be prevented. Fig. 7(b) shows that the 1EO-type phosphate ester exhibits the best dispersion ability for anti-agglomeration. The particle size measurements of such a high solid-content suspension (40 wt%) can only be directly analyzed by using an acoustic-type particle sizer.

3.3. Effect of particle size

The effect of particle size of $BaTiO_3$ powders on characteristics of suspensions was investigated. Table 2 compares the sedimentation time for the suspension containing 40 wt% $BaTiO_3$ powders (50 nm or 200 nm) in 1-methoxy-2-propanol, with 0–5 wt% surfactant (w.r.t. powders). It is expected that the 200 nm-$BaTiO_3$ suspension sediments more rapidly than the

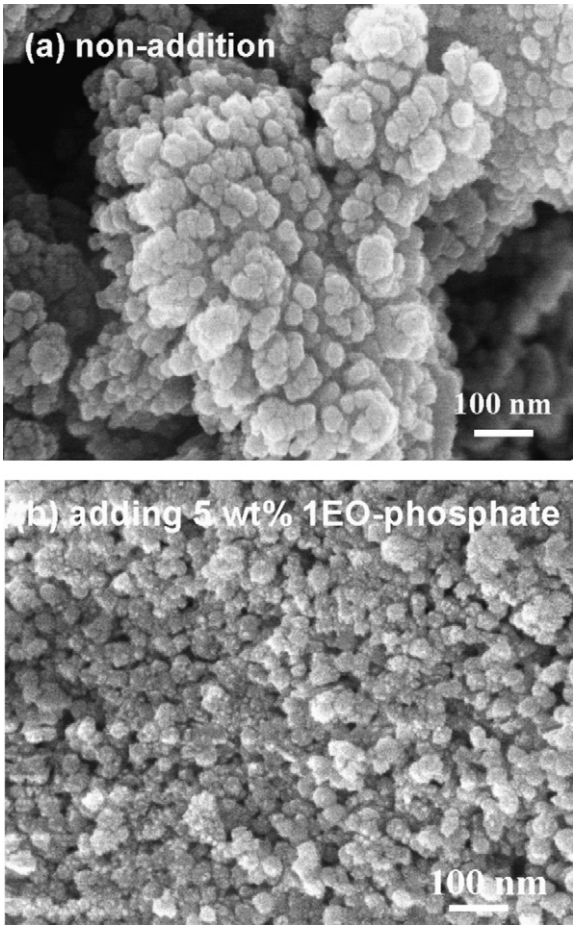

Fig. 6. SEM observation of dispersion effect on the $BaTiO_3$ powders with high solid content (40 wt%) due to 2-ethoxy ethyl dihydrogen (1EO-) phosphate addition in 1-methoxy-2-propanol: (a) non-addition and (b) added 5 wt%.

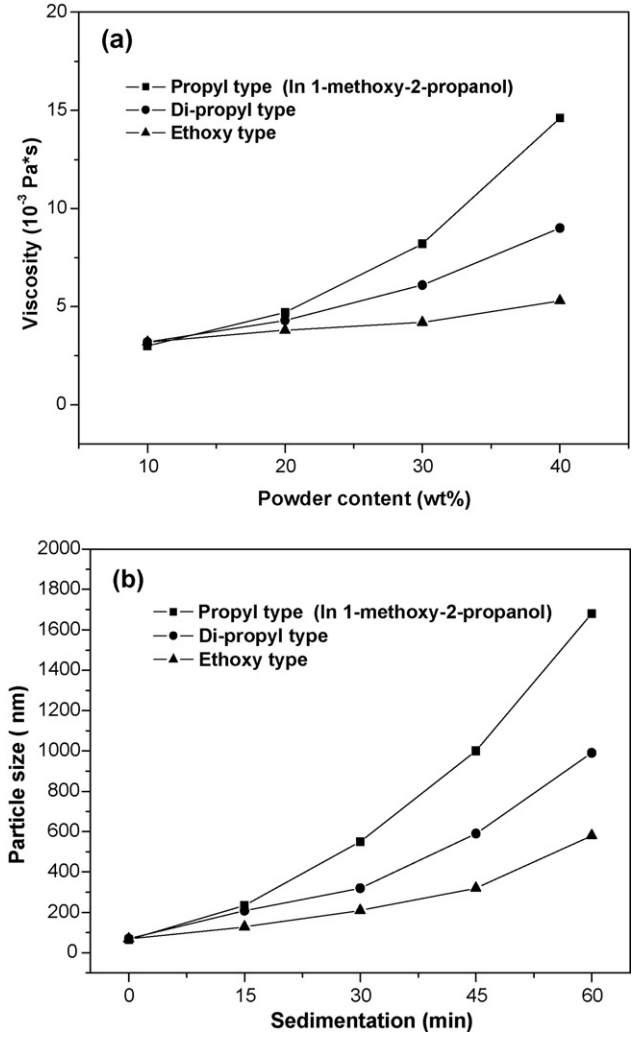

Fig. 7. The rheological behaviors of suspensions: (a) the viscosity of suspensions with different powder content by using three kinds of phosphate esters (3C, Di-3C and 1EO-) in 1-methoxy-2-propanol; (b) the variation of particle size measurements of high solid-content suspensions (40 wt%).

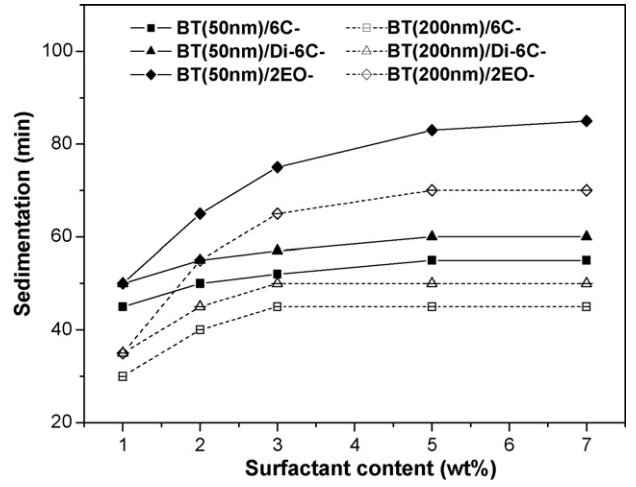

Fig. 8. Variation of sedimentation time for the smaller-sized $BaTiO_3$ suspension (50 nm, solid curves) and the larger-sized $BaTiO_3$ suspension (200 nm, dotted curves), which were added with various amount of surfactants.

50 nm-$BaTiO_3$ one when no surfactant was added. This table indicates the increasing sedimentation time after the phosphate esters addition. Moreover, the 200 nm-$BaTiO_3$ containing suspension favors the long carbon-chain phosphate esters, the 50 nm $BaTiO_3$ disperses better in the suspension when the shorter carbon-chain phosphate esters (3C-, Di-3C- or EO-) were used as surfactants.

The variation of sedimentation time with the surfactant content is shown in Fig. 8. From this figure, the optimal addition of surfactant can be obtained according to the plateau of sedimentation. The 200 nm-$BaTiO_3$ particles (dotted curves) need smaller amount of phosphate ester (2–3 wt%) to reach the ultimate dispersion. The probable explanation is that the specific surface area of 200 nm $BaTiO_3$ powders (5–8 m^2/g) is smaller than that of the 50 nm $BaTiO_3$ powders (15–18 m^2/g) and the zeta potential of 200 nm-$BaTiO_3$ powders in 1-methoxy-2-propanol (3.12 mV) is also smaller than that of the 50 nm-$BaTiO_3$ powders (4.05 mV). The ethoxy type phosphate ester results in longest sedimentation time among these three surfactants, that is, this phosphate ester shows most prominent improvement on dispersing the $BaTiO_3$ particles.

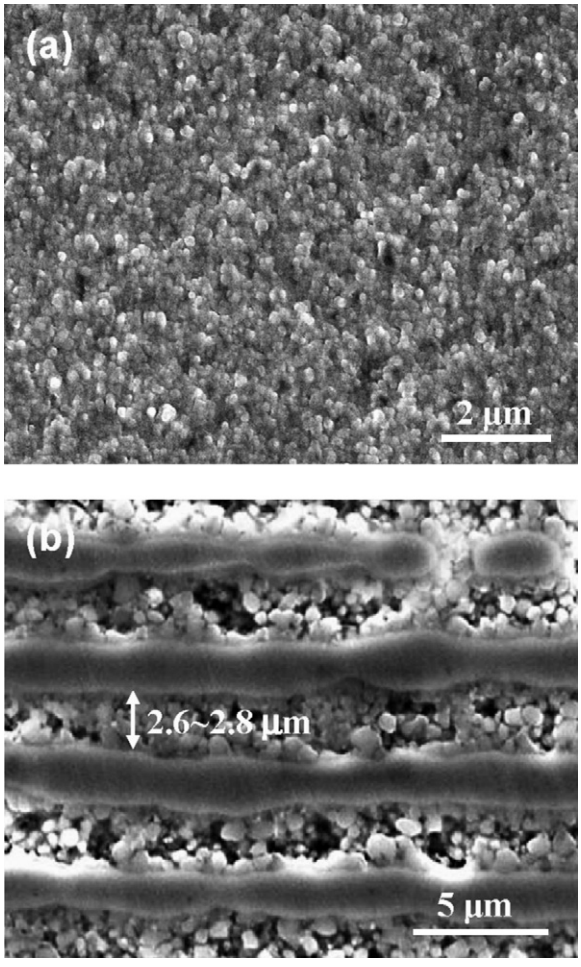

Fig. 9. The SEM micrograph of (a) surface of ultra-thin ceramic tape, which was prepared by tape-casting process using nano-$BaTiO_3$ (40 wt%) slurry added 2-ethoxy ethyl dihydrogen (1EO-) phosphate (5.0 wt% to $BaTiO_3$) in 1-methoxy-2-propanol; (b) cross-section of green MLCC device.

Table 3
The characteristics of the MLCC made of 50 nm-$BaTiO_3$ and 200 nm-$BaTiO_3$ powder slurry

Powder	Sintering	Stacking layers	Layer thickness	Grain size	Capacitance	Breakdown voltage
BT (200 nm)	1300 °C/2 h	10	2.2 μm	1.5 μm	102.1 ± 3 nF	94 ± 3 V
BT (50 nm)	1300 °C/2 h	10	2.4 μm	0.6 μm	116.9 ± 4 nF	108 ± 5 V

3.4. Multilayer ceramic capacitor based on nano-sized $BaTiO_3$ powders

The multilayer ceramic capacitors were then fabricated. The stable suspension was first prepared, using the 50 nm-$BaTiO_3$ (40 wt%) and 2-ethoxy ethyl dihydrogen (1EO-) phosphate esters (5 wt% w.r.t. $BaTiO_3$) in 1-methoxy-2-propanol. The organic additives, PVB & DOP, were added to adjust the viscosity of slurry to a suitable level (~250 cp) for tape casting. Typical surface of green ceramic foil and cross-sectional morphologies of the green MLCC devices are shown in Fig. 9(a) and (b), respectively. It should be noted that the $BaTiO_3$ powders were densely packed while the porous status in unsintered samples (shown as Fig. 9(b)) was caused by the loss of powders during polishing of the sample preparation. The supporting evidence of above mention is owing to Fig. 10(a), which illustrates the dense microstructure of the 1300 °C/2 h-sintered MLCC devices.

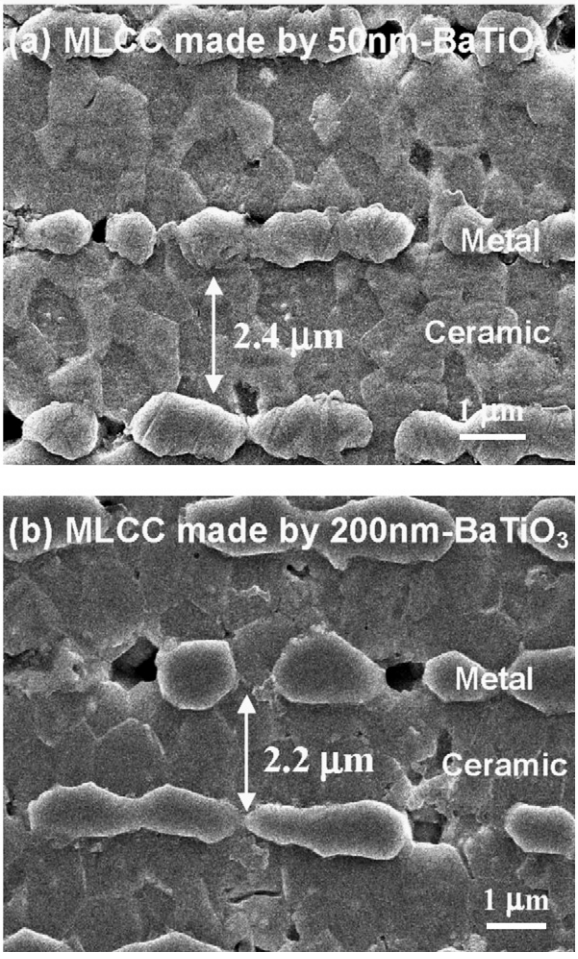

Fig. 10. SEM micrograph of sintered MLCC made of (a) 50 nm $BaTiO_3$ and (b) 200 nm $BaTiO_3$, where these slurries contain 40 wt% $BaTiO_3$ and appropriate surfactant in 1-methoxy-2-propanol.

After sintering, the 50-nm $BaTiO_3$ made MLCC devices contain layers about 2.4 μm in thickness. The $BaTiO_3$ grains are about 0.6 μm in size and are distributed very uniform (Fig. 10(a)). In contrast, SEM micrograph in Fig. 10(b) indicates that, for the MLCC made of 200 nm-$BaTiO_3$, the thickness of the $BaTiO_3$ layer is around 2.2 μm with much larger grains (~1.5 μm). Table 3 reveals that the capacitance value of 50 nm-$BaTiO_3$ based MLCC devices (116.9 nF) is markedly larger than the 200 nm-$BaTiO_3$ based ones (102.1 nF). Furthermore, the breakdown characteristic of the MLCC devices based on 50 nm-BaTiO3 powders (breakdown voltage, V_{BD} = 108 V) is superior to the ones based on 200 nm-$BaTiO_3$ powders (V_{BD} = 94 V). Apparently, the beneficial effect resulted from the utilization of nano-sized $BaTiO_3$ powders due to the smaller grain size of the correspondingly sintered device.

4. Conclusions

The factors affecting the dispersion of the nano-sized $BaTiO_3$ powders in non-aqueous media with different kinds of phosphate esters were investigated. The viscosity of solvent is the major factor that influences the dispersion behavior for suspension. Therefore, we utilized 1-methoxy-2-propanol to replace ethanol as solvent in this study. With the addition of phosphate esters, the sedimentation time was markedly increased. Among the phosphate esters studied, the 2-ethoxy ethyl dihydrogen (1EO-) phosphate esters showed the best dispersion behavior, which results in the longer sedimentation time for the 50 nm-$BaTiO_3$ containing suspension. Multilayer ceramic capacitors were fabricated by using a thin ceramic layer (2.6–2.8 μm) made of the nano-sized $BaTiO_3$ containing suspension. The 50-nm $BaTiO_3$-based MLCC devices possess the larger capacitance and superior breakdown voltage than 200-nm $BaTiO_3$ based ones, which is attributed to the small grains contained in this device.

References

[1]. Yao, K. and Zhu, W., Barium titanate glass-ceramic thin films for integrated high-dielectric media. *Thin Solid Films*, 2002, **408**(1–2), 11–14.
[2]. Schiom, D. G., Haeni, J. H., Lettieri, J., Thesis, C. D., Tian, W., Jiang, J. C. and Pan, X. Q., Oxide nano-engineering using MBE. *Mater. Sci. Eng. B-Solid.*, 2001, **B37**(3), 282–291.
[3]. Liu, D. M., Adsorption and Rheology, Packing, and sintering of nanosize ceramic powders. *Ceram. Int.*, 1999, **25**(2), 107–113.

[4]. Tseng, W. J. and Lin, C. L., Effect of dispersants on rheological behavior of batio$_3$ powders in ethanol–isopropanol mixtures. *Mater. Chem. Phys.*, 2003, **80**(1), 232–238.

[5]. Jean, J. H. and Wang, H. R., Effects of solids loading, pH, and polyelectrolyte addition on the stabilization of concentrated aqueous $BaTiO_3$ suspensions. *J. Am. Ceram. Soc.*, 2000, **83**(2), 277–280.

[6]. Wang, X. Y., Lee, B. I. and Mann, L., Dispersion of barium titanate with polyaspartic acid in aqueous media. *Colloids Surf. A*, 2002, **202**(1), 71–80.

[7]. Paik, U., Hackley, V., Choi, S. and Jung, Y., The effect of electrostatic repulsive forces on the stability of $BaTiO_3$ particles suspended in non-aqueous media. *Colloids Surf. A*, 1998, **135**(1–3), 77–88.

[8]. Paik, U. and Hackley, V., Influence of solids concentration on the isoelectric point of aqueous barium titanate. *J. Am. Cream. Soc.*, 2000, **83**(10), 2381–2384.

[9]. Bergstrom, L., Shinozaki, K., Tomiyama, N. and Mizutani, N., Colloidal processing of a very fine $BaTiO_3$ powder—effect of particle interactions on the suspension properties, consolidation, and sintering behavior. *J. Am. Ceram. Soc.*, 1997, **80**(2), 291–300.

[10]. Song, Y. L., Liu, X. L. and Chen, J. F., The maximum solid loading and viscosity estimation of ultra-fine $BaTiO_3$ aqueous suspensions. *Colloids Surf. A*, 2004, **247**(1–3), 27–34.

[11]. Shen, Z. G., Chen, J. F., Zou, H. K. and Yun, J. J., Dispersion of nanosized aqueous suspensions of barium titanate with ammonium polyacrylate. *J. Colliod Interf. Sci.*, 2004, **275**(1), 158–164.

[12]. Zhang, J. X., Jiang, D. L., Weisensel, L. and Greil, P., Deflocculants for tape casting of TiO_2 slurries. *J. Eur. Cream. Soc.*, 2004, **24**(8), 2259–2265.

[13]. Hsu, C. J. and Jean, J. H., Formulation dispersion of NiCuZn ferrite paste. *Mater. Chem. Phys.*, 2003, **78**(2), 323–329.

[14]. Reddy, S. B., Singh, P. P., Ranghu, N. and Kumar, V., Effect of type of solvent and dispersant on nano-PZT powder dispersion for tape casting slurry. *J. Mater. Sci.*, 2002, **37**(5), 929–934.

[15]. Gutierrez, C. A. and Moreno, R., Tape casting of non-aqueous silicon nitride slips. *J. Eur. Ceram. Soc.*, 2000, **20**(10), 1527–1537.

[16]. Boch, P., Chartier, T. and Huttepain, M., Tape casting of Al_2O_3/ZrO_2 laminated composites. *J. Am. Ceram. Soc.*, 1986, **69**(8), 191–192.

[17]. Lebars, N., Levitz, P., Messier, A., Francois, M., Vandamme, H. and Deagglomeration, Dispersion of barium–titanate and alumina powders in an organic medium. *J. Colliod. Interf. Sci.*, 1995, **175**(2), 400–410.

[18]. Chartier, T., Jorge, E. and Boch, P., Dispersion properties of $BaTiO_3$ tape-casting slurries. *J. Eur. Ceram. Soc.*, 1993, **11**(5), 389–393.

[19]. Mikeska, K. R. and Cannon, W. R., Non-aqueous dispersion properties of pure barium–titanate for tape casting. *Colloids Surf.*, 1988, **29**(3), 305–321.

[20]. Chartier, T., Streicher, E. and Boch, P., Phosphate-esters as dispersants for the tape casting of alumina. *Am. Ceram. Soc. Bull.*, 1987, **2**(4), 1653–1655.

[21]. Nelson, A. K. and Toy, A. D., The preparation of long-chain monoalkyl phosphates from pyrophosphoric acid and alcohols. *Inorg. Chem.*, 1963, **2**, 775–777.

[22]. Romsted, L. S. and Yoon, C. O., Counterion affinity orders in aqueous micellar solutions of sodium decyl phosphate and sodium dodecyl-sulfate determined by changes in Na-23 NMR relaxation rates—a surprising dependence on head group charge. *J. Am. Chem. Soc.*, 1993, **115**(3), 989–994.

[23]. Jean, J. H. and Wang, H. R., Stabilization of aqueous $BaTiO_3$ suspensions with ammonium salt of poly(acrylic acid) at various pH values. *J. Mater. Res.*, 1998, **13**(8), 2245–2250.